

E15-2002-157

MEASUREMENT  
OF THE TEMPERATURE DEPENDENCE  
OF THE  $dd_{\mu}$  MOLECULE FORMATION RATE  
IN DENSE DEUTERIUM  
AT TEMPERATURES 85–790 K

Submitted to «ЖЭТФ»

V. R. Bom<sup>1</sup>, D. L. Demin, C. W. E. van Eijk<sup>1</sup>, V. V. Filchenkov, N. N. Grafov,  
V. G. Grebinnik, K. I. Gritsaj, A. D. Konin, A. V. Kuryakin<sup>2</sup>, V. A. Nazarov<sup>2</sup>,  
V. V. Perevozchikov<sup>2</sup>, A. I. Rudenko, S. M. Sadetsky<sup>3</sup>, Yu. I. Vinogradov<sup>2</sup>,  
A. A. Yukhimchuk<sup>2</sup>, S. A. Yukhimchuk, V. G. Zinov, S. V. Zlatoustovskii<sup>2</sup>

---

<sup>1</sup>Delft University of Technology, 2629 JB Delft, the Netherlands

<sup>2</sup>Russian Federal Nuclear Center, All-Russian Research Institute of Experimental Physics (RFNC–VNIIEF), Sarov, Nizhny Novgorod Region, Russia

<sup>3</sup>St. Petersburg Nuclear Physics Institute (PNPI), Gatchina, Russia

# 1 Motivation

The processes of Muon Catalyzed Fusion (MCF) in deuterium were studied in many laboratories [1-10]. Recent years have seen significant success both in theoretical consideration [11-14] and in the measurements of the  $dd\mu$  molecule formation rate including strong spin effects. Recent data [9, 10] give an example of the progress achieved in the accuracy of measuring the fine effects of MCF in low-density deuterium gas at temperatures  $28 \div 350$  K. But there are still no direct experimental data for the MCF processes at temperatures above 400 K. The only experimental result (non-direct) of  $\lambda_{dd\mu}$  at temperatures up to 600 K [2] was obtained from analysis of muon losses in the experiment with double deuterium-tritium mixtures and had big errors. It is important that at these temperatures one should expect [14] a large  $dd\mu$  formation rate for the  $d\mu$  atom spin state  $F = 1/2$  prevailing over that for the spin  $F = 3/2$ . Besides, this measurements of  $\lambda_{dd\mu}$  at high temperatures are necessary for correcting the evaluation of the parameters of the  $dt$  fusion cycle derived from the experiments [15].

Here we present the results of the measurements in a dense deuterium gas in a wide temperature range 85 – 790 K. The aim of the experiment was to measure the formation rate  $\lambda_{dd\mu}$  in dense deuterium for the first time in the temperature range up to 800 K. The scheme of the process is presented in Fig. 1.

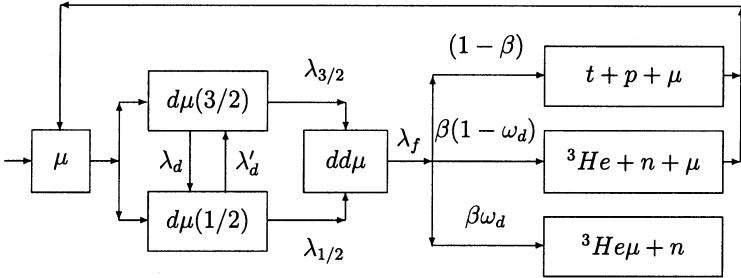
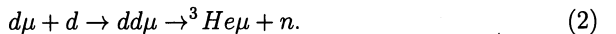
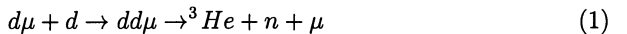


Fig.1. Scheme of the  $dd$  cycle.

# 2 Experiment

The experimental method is similar to that used in [16]. We measured and analyzed the time and charge (deposited energy in a neutron detector) distributions of 2.5 MeV neutrons from the  $dd$  fusion reactions



The simplified experimental lay-out is shown in Fig. 2. The essence of the experimental installation is described in [17]. The installation was mounted on the muon beam line of the JINR phasotron.

## 2.1 Target

The central part of the installation is a specially constructed deuterium high pressure target (T) [18] of volume  $76 \text{ cm}^3$ . The target is able to withstand pressures up to  $1500 \text{ bar}$  at temperatures up to  $800 \text{ K}$ . A set of devices [18] was used for handling the deuterium gas. To achieve the deuterium purity of impurities with  $Z > 1$  at a level of  $0.1 \text{ ppm}$  the target was filled by using a palladium filter and a vanadium-deuterium pressure source [19].

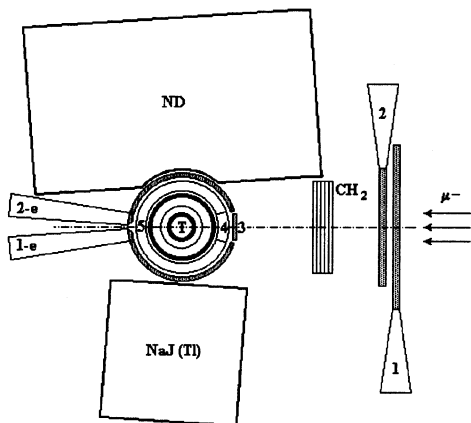


Fig. 2. Experimental lay-out.

## 2.2 Detectors

The target is surrounded by a set of detectors. Scintillation counters 1-3 detected incoming muons. Cylinder-shaped proportional counters 4 and 5 (analogous to [20]) served to select muon stops in the target (signal  $1 \cdot 2 \cdot 3 \cdot 4 \cdot 5$ ). Specially designed cylinder-shaped scintillation counters 1-e, 2-e were used to detect  $\mu$ -decay electrons. A coincidence between the signals of the counters 5 and 1-e, 2-e was considered as a  $\mu$ -decay electron. A large neutron detector ND (volume of  $NE - 213$  is equal to  $12.5 \text{ l}$ ) [21] was aimed to detect neutrons from reactions (1), (2). To reduce the background, the  $n - \gamma$  separation was realized by comparing the signals for the total light and the fast component light of the ND signal. The  $\gamma$ -quantum discrimination efficiency was better than  $10^{-3}$  for energies larger than  $100 \text{ keV}$ .

The  $NaI(Tl)$  crystal was used to search for the rare fusion channel  $d(d, \gamma)^4He$  in parallel to the main aim of the experiment (the subject matter of this paper). The results of this search will be published elsewhere [22].

The timing sequence of the 4, 5, 1-e, 2-e and ND signals was registered by flash ADC and was recorded on the PC. The trigger is described in [23].

### 2.3 Experimental conditions

Two exposure runs were carried out. One was with a target filled with an equilibrium protium-deuterium mixture (21% of  $H$ ) in the temperature range 85 – 300  $K$  at the density  $\varphi \simeq 0.84$   $LHD$  (as usual, density is given in units of liquid hydrogen density,  $LHD = 4.25 \cdot 10^{22}$   $nucl/cm^3$ ). The exposure at  $\varphi \simeq 0.47$   $LHD$  was also measured at a temperature of 300  $K$ .

The other exposure run was carried out with a target filled with pure deuterium (protium content was about 0.1%) in the temperature range 300 – 790  $K$  at the density  $\varphi \simeq 0.48$   $LHD$ .

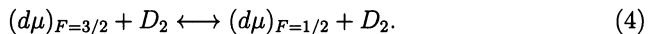
The experimental conditions and the gathered electron statistics for all runs are presented in Table 1. The background exposure with empty target was also carried out.

Table 1. Experimental conditions and statistics.

Run	T, K	Content, %		$\varphi$ , $LHD$	$N_e$
		H	D		
1	85 (1)	20.7 (0.1)	79.3 (0.5)	0.840 (0.025)	685 200
2	110 (1)	20.7 (0.1)	79.3 (0.5)	0.841 (0.025)	456 500
3	230 (1)	20.7 (0.1)	79.3 (0.5)	0.831 (0.025)	415 900
4	301 (3)	20.7 (0.1)	79.3 (0.5)	0.831 (0.025)	427 000
5	299 (3)	20.7 (0.1)	79.3 (0.5)	0.473 (0.014)	374 900
6	290 (4)	0.1 (0.1)	99.9 (0.1)	0.480 (0.014)	355 500
7	401 (10)	0.1 (0.1)	99.9 (0.1)	0.480 (0.014)	226 900
8	530 (10)	0.1 (0.1)	99.9 (0.1)	0.480 (0.014)	194 900
9	660 (10)	0.1 (0.1)	99.9 (0.1)	0.480 (0.014)	208 700
10	791 (15)	0.1 (0.1)	99.9 (0.1)	0.483 (0.020)	301 900

### 3 Kinetics of the $dd\mu$ fusion cycle

The basic processes of the kinetics of the resonant formation of  $dd\mu$  molecules are considered in [11, 12]. The  $d\mu$  atoms are formed during the time  $\sim 10^{-12} \cdot \varphi^{-1}$  s [24] with an energy of a few eV and thermalized with the rate  $\sim 10^9 \cdot \varphi$  s $^{-1}$  [25]. Two different hyperfine states of the  $d\mu$  atoms  $F = 3/2$  and  $F = 1/2$  are statistically populated with the probabilities 2/3 and 1/3 respectively. After that the processes of resonant  $dd\mu$  formation (3) and  $d\mu$  atom spin-flip processes (4) take place



The rates of direct and inverse spin-flip processes (4) ( $\lambda_d$  and  $\lambda'_d$ ) are connected by the detailed balance relation:

$$\lambda'_d = \gamma \cdot \lambda_d, \quad \gamma = 2 \cdot \exp(-\Delta E/T), \quad \Delta E = 0.0485 \text{ eV}. \quad (5)$$

In the process of the resonant  $dd\mu$  formation (3) the released energy (the binding energy of the formed  $dd\mu$  mesomolecule) is transmitted to the excitation of vibration-rotational states of the mesic molecular complex  $[(dd\mu)dee]^*$ . In the case of the usually nonresonant  $dd\mu$  formation (6)



the released energy is taken away by a conversion electron. The rate of this nonresonant mechanism ( $\lambda_{nr}$ ) is sufficiently small and rises with temperature (energy) as [26]

$$\lambda_{nr} = \lambda_1 + \lambda_2 \cdot (3/2)kT, \quad \lambda_1 = 0.04 \mu s^{-1}, \quad \lambda_2 = 2.3 \mu s^{-1} \cdot eV^{-1}. \quad (7)$$

In the formed  $dd\mu$  complex (3) the processes of  $dd$  fusion (with rates  $\lambda_f \sim 10^9 s^{-1}$  [27])



compete with the processes of complex deexcitation and complex back decay. The  $d\mu$  atom formation rate and the thermalization rate as well as the  $dd$  fusion rate are much higher than the effective hyperfine transition rates and the effective (experimentally observable) mesomolecule formation rate. So at times larger than the lifetime ( $\sim 0.5 \text{ ns}$ ) of the mesomolecular complex the kinetics is described by the scheme shown in Fig. 1 and depends on the effective rates of spin-flip processes (4) and the effective rates of  $dd\mu$  formation from two hyperfine states ( $\lambda_{1/2}$  and  $\lambda_{3/2}$ ). The following system of differential equations corresponds to the kinetics of Fig. 1 [11, 28]

$$dN_{3/2}/dt = -(\lambda_0 + \lambda_d + \lambda_{3/2})N_{3/2} + 2/3(1-w)\lambda_{3/2}N_{3/2} + [2/3(1-w)\lambda_{1/2} + \lambda'_d]N_{1/2} \quad (11)$$

$$dN_{1/2}/dt = -(\lambda_0 + \lambda'_d + \lambda_{1/2})N_{1/2} + 1/3(1-w)\lambda_{1/2}N_{1/2} + [1/3(1-w)\lambda_{3/2} + \lambda_d]N_{3/2} \quad (12)$$

$$dN_n/dt = \beta \cdot \varphi \cdot (\lambda_{3/2}N_{3/2} + \lambda_{1/2}N_{1/2}) \quad (13)$$

Here  $N_{3/2}$ ,  $N_{1/2}$  are populations of the  $F = 3/2$  and  $F = 1/2$   $d\mu$  atom hyperfine states;  $N_n$  is the number of fusion neutrons;  $w = \beta w_d$ ,  $\beta$  is the probability of the

${}^3\text{He}$ -reaction channel (8) and (10),  $w_d = 0.13$  is the probability of muon sticking to  ${}^3\text{He}$  [11];  $\lambda_0$  is the muon decay rate.

This system of differential equations (11)-(13) was considered and its approximate solution was obtained [11, 28].

## 4 Analysis

The first step of the analysis of registered events consists in separation of neutrons,  $\gamma$ -quanta and  $\mu$ -decay electrons. Then for each exposure we build and analyze the time and charge (deposited energy in a neutron detector) distributions of fusion neutrons and the time distributions of  $\mu$ -decay electrons.

### 4.1 Electron time spectra

Time spectra of electrons after muon stops in the target were created and analyzed for each exposure including the background run with the empty target. The fitting of the background electron time spectra allows us to obtain the number of muon stops in the target walls. Then the numbers of electrons  $N_e$  from the muon stopped in deuterium were obtained for each exposure. They were necessary for normalization. A typical example of the fitted time distributions of decay electrons for the deuterium-filled target is shown in Fig. 3. The dashed line corresponds to the electrons from decays of muons stopped in the target walls (empty target).

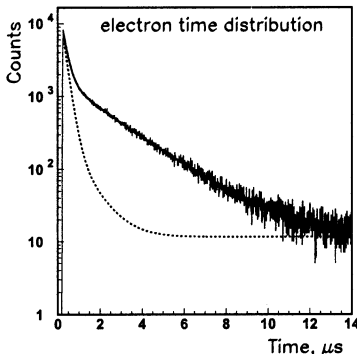


Fig. 3. Example of the experimental time spectrum of electrons from  $\mu$ -decay. Solid line is the fitting function. Dashed line corresponds to the empty target.

The observed muon disappearance rates are in agreement with the muon decay rate  $\lambda_0 = 0.455 \mu\text{s}^{-1}$  with an accuracy not worse than 1.5%.

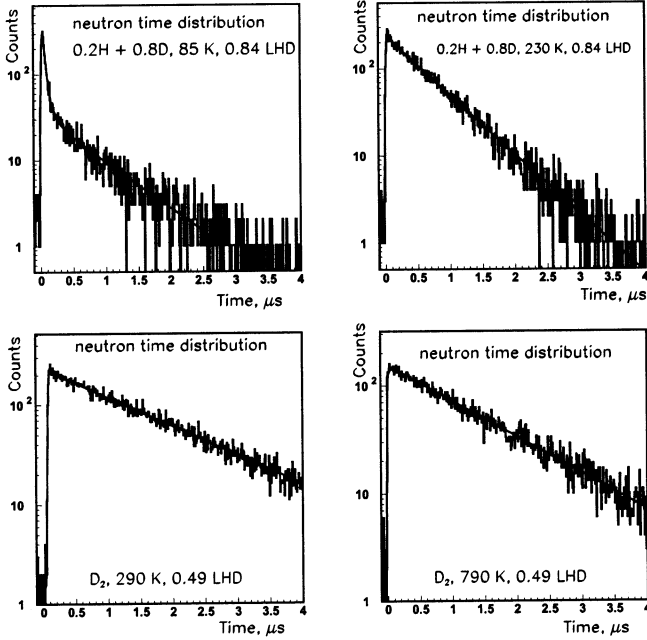


Fig. 4. Experimental time spectra of fusion neutrons measured for exposures at temperatures 85, 230, 290 and 790 K. Solid lines are the fitting functions.

## 4.2 Neutron time and charge spectra

Only the first detected neutrons were selected for the analysis. To reduce the background the time selection criterion [29]

$$t_n + 0.5 \mu s < t_e < t_n + 4.5 \mu s, \quad (14)$$

was used, where  $t_n$  and  $t_e$  are neutron and electron detection times measured from the moment of muon stop in the target. The time and charge (energy) distributions were plotted for these events. Examples of the time distributions of fusion neutrons are shown in Fig. 4 for four temperatures.

According to [11, 28], the solution of the system of differential equations (11)-(13) the time distributions of the first neutrons detected with the efficiency  $\epsilon$  have the form of the sum of two exponents:



$$N_n(t) = A_{fast} \cdot \exp(-\lambda_{fast}t) + A_{slow} \cdot \exp(-\lambda_{slow}t). \quad (15)$$

The parameters of this expression are the functions of  $\lambda_d$ ,  $\lambda_{1/2}$ ,  $\lambda_{3/2}$  and  $\alpha \equiv \epsilon + \omega - \epsilon\omega$ . They can be reconstructed from the amplitudes and slopes of the exponents of expression (15). The amplitude of the first term of (15)  $A_{fast}$  is related to the  $dd\mu$  formation from the  $d\mu$  atom with spin  $F = 3/2$  and its slope  $\lambda_{fast}$  is determined mainly by the value of  $\lambda_d$ . The amplitude of the second term (slow component) corresponds to the so-called steady state of the  $dd\mu$  cycle. The steady state  $dd\mu$  formation rate  $\lambda_{ss}$  presents the "mean" value of the  $dd\mu$  formation rate from different  $d\mu$  spin states for times  $t > \lambda_{fast}^{-1}$ . The ratio of amplitudes  $A_{fast}/A_{slow}$  is responsible for the ratio  $\lambda_{3/2}/\lambda_{1/2}$ .

The values of  $\lambda_{ss}$  were obtained from

$$\lambda_{ss} = \frac{\lambda_n}{\varphi\beta} \cdot \frac{N_n}{N_e\epsilon f_t}. \quad (16)$$

Here the second ratio means the absolute neutron yield for the steady state of the  $dd$  cycle,  $\lambda_n$  is the slow exponent slope of (15),  $N_n$  is the number of fusion neutrons. The time selection factor  $f_t = 0.67$  is due to criterion (14).

Determination of the neutron detection efficiency  $\epsilon$  is analogous to that in [30]. To determine the efficiency loss due to the finite energy threshold, the calculated recoil proton energy spectrum was reconciled with the experimental energy distribution. This procedure was done for each exposure, its example is given in Fig. 5. The line in the figure is the calculated response function of the ND and the histogram is the experimental energy distribution. The efficiency of the ND is obtained to be  $\simeq 12\%$  and its accuracy is about 8%.

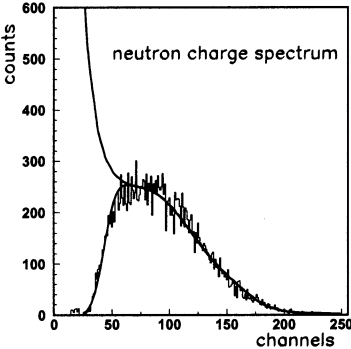


Fig. 5. Neutron energy distribution. The histogram is the experimental neutron energy distribution. The line is the calculated response function of the ND.

The fit strategy was as follows. At the first step we fitted only the slow part of the neutron time spectra and found the steady state formation rates ( $\lambda_{ss}$ ) using expression (16). At the next step we fitted the whole neutron time spectra using formula (15). In this fit formula (15) was convolved with a Gaussian resolution function to allow for the finite time resolution and to determine the time zero position. The analysis showed that the time zero stability during the data taking was better than 0.5 ns. The background due to muon stops in the target walls and due to accidental coincidence was taken into account in the fit procedure. At the final step of the analysis the values of  $\lambda_{3/2}$ ,  $\lambda_{1/2}$  and  $\lambda_d$  were obtained from the values of  $\lambda_{ss}$  and parameters of expression (15). The method developed in [28] was used for this purpose.

We made some corrections to the final values of the rates which are due to the nonresonant  $dd\mu$  formation rate on molecules  $D_2$  and  $HD$  [31] (in runs with double H/D mixtures).

It turned out that the reliable separation of fast and slow terms of (15) in fitting is possible only at low temperatures (in our case not higher than 290 K), where the rates of  $\lambda_{3/2}$  and  $\lambda_{1/2}$  are essentially distinguished and  $\lambda_d$  is much larger than  $\lambda'_d$ . At high temperatures (higher than 300 K) the rates of  $\lambda_{3/2}$  and  $\lambda_{1/2}$  are approximately equal [14] and so it is a great problem in fits to obtain the fast component parameters and thus to distinguish the values of  $\lambda_{3/2}$  and  $\lambda_{1/2}$ . At this temperatures we obtained only the value of  $\lambda_{ss}$ . As for  $\lambda_d$  which is determined from the fast exponent slope, we obtained its value only at the temperatures 85 and 110 K for the same reasons.

## 5 Results and discussions

The obtained values of  $\lambda_{ss}$ ,  $\lambda_d$ ,  $\lambda_{3/2}$  and  $\lambda_{1/2}$  are presented in Tables 2,3. All rates are normalized to the LHD. The statistic error is 2 – 3%. The main sources of systematic errors are the uncertainties of the ND efficiency ( $\simeq 8\%$ ) and gas density ( $\simeq 3\%$ ).

Table 2. Experimental results for the steady state  $dd\mu$  formation rate.

$T, K$	$\lambda_{ss}, \mu s^{-1}$		
	Value	Stat. error	Syst. error
85	0.197	0.007	0.018
110	0.485	0.015	0.044
230	2.06	0.06	0.19
301	2.69	0.08	0.24
299	2.57	0.08	0.24
290	2.67	0.08	0.24
401	3.00	0.09	0.27
530	3.10	0.09	0.27
660	2.67	0.08	0.24
791	2.30	0.07	0.21

In Fig. 6 the temperature dependence  $\lambda_{ss}(T)$  is shown together with the data [2]. The main result of this work is the direct measurement of the steady state  $dd\mu$  formation rate at temperatures above 400 K. As is seen, our data are in good agreement with the theoretical predictions [14] at low temperatures (up to 400 K). But at high temperatures the experimental data are slightly larger than the theoretical ones.

Table 3. Experimental results for the effective  $dd\mu$  formation rates from different spin states and the effective  $d\mu$  spin-flip rate.

$T, K$	$\lambda_{1/2}, \mu s^{-1}$			$\lambda_{3/2}, \mu s^{-1}$			$\lambda_d, \mu s^{-1}$		
	Value	Stat. error	Syst. error	Value	Stat. error	Syst. error	Value	Stat. error	Syst. error
85	0.170	0.006	0.015	4.63	0.13	0.42	32.8	1.0	3.2
110	0.403	0.014	0.036	4.79	0.14	0.43	31.4	1.2	3.2
230	1.72	0.06	0.16	3.92	0.12	0.35	–		
290	2.40	0.08	0.22	3.52	0.10	0.32	–		

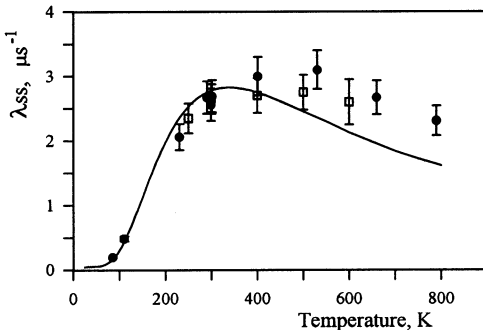


Fig. 6. Values of  $\lambda_{ss}$  as a function of temperature. Circles are our data, squares are the LAMPF data [2]. The line is the theory [14].

In Fig. 7 the temperature dependence of  $\lambda_{1/2}$  and  $\lambda_{3/2}$  is shown. The solid line is theoretical calculations [14]. The values of  $\lambda_d$ ,  $\lambda_{1/2}$  and  $\lambda_{3/2}$  are in good agreement with theory and with other experimental data [9, 10, 17].

As was mentioned above, under our experimental conditions the reliable separation of fast and slow terms of (15) in fitting and thus obtaining of values  $\lambda_d$ ,  $\lambda_{1/2}$  and  $\lambda_{3/2}$  is possible only at low temperatures. The lifetime of the fast component of neutron spectra (15) is  $\tau = 1/\lambda_{fast} \sim 1/(\lambda_d\varphi)$ . Under our conditions ( $\varphi \simeq 0.5 LHD$ ) it equals  $\sim 50 ns$  or about five channels in the measured time histogram. This fact is confirmed also by our Monte-Carlo calculations. So it is worth carrying out the experiment at high temperatures with deuterium of low density (about 0.05 LHD) where the spin effect time range at neutron time distributions will be about 0.5  $\mu s$ . Such kind of experiment could be conducted at a muon-factory.

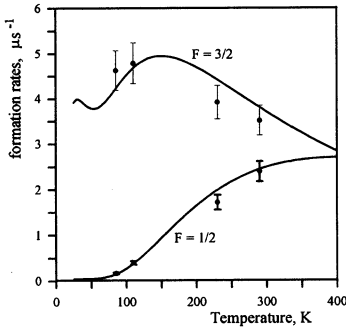


Fig. 7. Values of  $\lambda_{3/2}$  and  $\lambda_{1/2}$  as a function of temperature. Lines are the theory [14].

## 6 Conclusions

The first direct measurements of the MCF  $dd$  fusion cycle parameters at high temperatures (up to 790 K) are carried out. The values of the steady state  $dd\mu$  formation rate are obtained for the entire temperature range. The comparison with theory showed good agreement at low temperatures (up to 400 K) and some difference at high temperatures (above 400 K). At low temperatures the values of effective rates  $\lambda_{3/2}$ ,  $\lambda_{1/2}$  are obtained, they are in agreement with theory. To measure these hyperfine parameters in the high temperature range seems to require an experiment of special sort, i.e. at low deuterium density ( $\sim 0.01 - 0.05$  LHD) with a high-intensity muon beam.

The authors are grateful to Prof. L.I. Ponomarev, M.P. Faifman, N.I. Voropaev for the discussions. We also wish to thank M.M. Petrovsky, A.P. Kustov and the staff of the RFNC-VNIIEF group for their help in tests and runs. The work was supported by the Ministry of Atomic Energy of the RF (treaty No 6.25.19.19.99.969) and the Ministry of Science and Technology of the RF (state contract No 103-7(00)-II) and the RFBR (Project 01-02-16425).

## References

- [1] V.M. Bystritsky et al., Zh. Eksp. Teor. Fiz. **76**, 460 (1979).
- [2] S.E. Jones et al., Phys. Rev. Lett. **56**, 588 (1986).
- [3] D.V. Balin et al., Pis'ma Zh. Eksp. Teor. Fiz. **40**, 318 (1984).
- [4] D.V. Balin et al., Muon Cat. Fusion **2**, 241 (1988).
- [5] J. Zmeskal et al., Muon Cat. Fusion **1**, 109 (1987).
- [6] N. Nagele et al., Nucl. Phys. A **493**, 397 (1989).

- [7] V.M. Bystritsky et al., *Muon Cat. Fusion* **5/6**, 141 (1990/91).
- [8] D.V. Balin et al., *Muon Cat. Fusion* **5/6**, 163 (1990/91).
- [9] C. Petitjean et al., *Hyp. Int.* **118**, 127 (1999).
- [10] D.V. Balin et al., proceedings of the conference  $\mu CF - 01$ , Japan, Shimoda, April 22-26, 2001 year.
- [11] M.P. Faifman et al., *Zh. Exp. Teor. Fiz.* **92**, 1173 (1987); *Sov. Phys. JETP* **65**, 656 (1987).
- [12] M.P. Faifman, *Muon Cat. Fusion* **2**, 247 (1988); M.P. Faifman, L.I. Menshikov and T.A. Strizh, *Muon Cat. Fusion* **4**, 1 (1989).
- [13] A. Scrinzi, *Muon Cat. Fusion* **5/6**, 179 (1990).
- [14] M.P. Faifman, *Hyp. Int.* **101/102**, 179 (1996).
- [15] V.R. Bom et al., proceedings of the conference  $\mu CF - 01$ , Japan, Shimoda, April 22-26, 2001 year.
- [16] Yu.P. Averin et al., *Hyp. Int.* **118**, 111 (1999).
- [17] V.P. Dzhelepov et al., *Zh. Eksp. Teor. Fiz.* **101**, 1105 (1992); *Muon Cat. Fusion* **7**, 387 (1992).
- [18] V.V. Perevozchikov et al., proceedings of the conference  $\mu CF - 01$ , Japan, Shimoda, April 22-26, 2001 year.
- [19] A.N. Golubkov and A.A. Yukhimchuk, proceedings of the conference  $\mu CF - 01$ , Japan, Shimoda, April 22-26, 2001 year.
- [20] A.D. Konin, Preprint JINR **P13-82-634** (1982).
- [21] V.P. Dzhelepov et al., *Nucl. Instr. and Meth.*, **A 269**, 634 (1988).
- [22] L.N. Bogdanova et al., Preprint JINR **E15-2001-264** (2001); "Search for the radiative capture  $d+d \rightarrow {}^4He + \gamma$  from the  $dd\mu$  muonic molecule state", will be published in *Nucl. Phys.*, 2001.
- [23] V.G. Zinov, A.I. Rudenko, V.T. Sidorov, Preprint JINR **P13-96-439** (1996).
- [24] J.S. Cohen, *Phys. Rev. A* **27**, 167 (1983).
- [25] A. Adamchak and V.S. Melezhik, *Muon Cat. Fusion* **5/6**, 303 (1990).
- [26] S.I. Vinitzky et al., *Zh. Eksp. Teor. Fiz.* **74**, 849 (1978); *Sov. Phys. JETP* **47**, 444 (1978).

- [27] L.N. Bogdanova et al., Phys. Lett. **115 B**, 171 (1982).
- [28] V.V. Filchenkov, Preprint JINR **E1-89-57** (1989).
- [29] V.R. Bom et al., JETP **84(4)**, 641 (1997).
- [30] V.R. Bom and V.V. Filchenkov, Hyp. Int. **118**, 365 (1999).
- [31] G.G. Semenchuk et al., Hyp. Int. **118**, 141 (1999).

---

Received on July 5, 2002.

Бом В. Р. и др.

E15-2002-157

Измерение температурной зависимости от скорости образования  $dd\mu$ -молекул в плотном дейтерии при температурах 85–790 К

На фазотроне ОИЯИ проведено исследование процесса мюонного катализа в дейтерии. Измерения проводились с использованием дейтериевой мишени высокого давления в температурном диапазоне 85–790 К при плотностях  $\cong 0,5$  и  $0,8$  от плотности жидкого водорода. Представлены первые экспериментальные результаты для скорости образования  $dd\mu$ -молекулы в температурном диапазоне 400–790 К при плотности дейтерия  $\cong 0,5$  от плотности жидкого водорода.

Работа выполнена в Лаборатории ядерных проблем им. В. П. Дзелепова ОИЯИ.

Препринт Объединенного института ядерных исследований. Дубна, 2002

Bom V. R. et al.

E15-2002-157

Measurement of the Temperature Dependence of the  $dd\mu$  Molecule Formation Rate in Dense Deuterium at Temperatures 85–790 K

Muon catalyzed fusion (MCF) in deuterium was studied by the MCF collaboration at the JINR phasotron. The measurements were carried out with a high pressure deuterium target in the temperature range 85–790 K at densities  $\cong 0.5$  and  $0.8$  of liquid hydrogen density (LHD). The first experimental results for the  $dd\mu$ -molecule formation rate  $\lambda_{dd\mu}$  in the temperature range 400–790 K with deuterium density  $\cong 0.5$  LHD are presented.

The investigation has been performed at the Dzhelepov Laboratory of Nuclear Problems, JINR.

Preprint of the Joint Institute for Nuclear Research. Dubna, 2002

Макет *Т. Е. Попеко*

ЛР № 020579 от 23.06.97.

Подписано в печать 26.07.2002.

Формат 60 × 90/16. Бумага офсетная. Печать офсетная.

Усл. печ. л. 0,93. Уч.-изд. л. 1,0. Тираж 300 экз. Заказ № 53451.

Издательский отдел Объединенного института ядерных исследований  
141980, г. Дубна, Московская обл., ул. Жолио-Кюри, 6.